UDC 621.313 https://doi.org/10.20998/2074-272X.2024.4.01

A. Kimouche, M.R. Mekideche, M. Chebout, H. Allag

Influence of permanent magnet parameters on the performances of claw pole machines used in hybrid vehicles

Introduction. *Claw pole machines (CPM) are commonly used in the automotive industry. Recently, importance has focused on the use and introduction of permanent magnets (PM) in this type of machine to increase the power density. This paper studies the performance of permanent magnet claw pole machines (PM-CPM) used in hybrid electric vehicle applications. The structure considers that the PMs are placed between the claws of the rotor.* ***Purpose****. The influence of the PM magnetization effect on the performance of synchronous PM-CPM is analyzed. Radial and tangential magnetizations are applied to obtain the best possible sinusoidal shape of the electromotive force and an acceptable cogging torque. Then, the electromagnetic performance of the PM-CPM is analyzed and evaluated. Furthermore, due to the complexity of the rotor armature, it seems difficult to give a direct relationship between the PM parameters and the machine torque. This led us to study the effects of magnets geometrical dimensions variations on the torque and its ripple.* ***Method.*** *3D nonlinear model of the machine is analyzed using the finite element method and comparisons between some electromagnetic performances are processed.* ***Results****. It was found that the tangential magnetization of PMs makes it possible to obtain a better distribution of the flux density and a minimum of cogging torque mainly responsible for vibrations and acoustic noise. Also, we observed a non-linear variation between the torque and its ripples depending on the dimensions of the PM. In fact, electromagnetic torque increases linearly with PM size but this is not the case for torque ripples.* References 22, tables 2, figures 16.

Key words: **claw pole machine, permanent magnet dimension, hybrid electric vehicles, finite element method, torque ripple.**

Вступ*. Машини з нігтьовим полюсом (CPM) зазвичай використовуються в автомобільній промисловості. Останнім часом велика увага приділяється використанню та впровадженню постійних магнітів (PM) у машинах цього типу для збільшення питомої потужності. У цій статті вивчаються характеристики машин з нігтьовим полюсом із постійними магнітами (PM-CPM), що використовуються у гібридних електромобілях. У конструкції передбачено, що PM розміщуються між кулачками ротора.* ***Мета****. Проаналізовано вплив ефекту намагнічування PM на продуктивність синхронного PM-CPM. Радіальна та тангенціальна намагніченість застосовуються для отримання максимально можливої синусоїдальної форми електрорушійної сили та прийнятного зубчастого моменту. Потім аналізуються та оцінюються електромагнітні характеристики PM-CPM. Крім того, через складність якоря ротора здається скрутним встановити пряму залежність між параметрами PM і крутним моментом машини. Це спонукало вивчити вплив змін геометричних розмірів магнітів на крутний момент і його пульсації.* ***Метод****. Тривимірна нелінійна модель машини аналізується з використанням методу скінченних елементів та виконується порівняння деяких електромагнітних характеристик.* ***Результати****. Встановлено, що тангенціальне намагнічування PM дозволяє отримати кращий розподіл магнітної індукції та мінімуму зубчастого моменту, відповідального головним чином за вібрації та акустичний шум. Також ми спостерігали нелінійну зміну крутного моменту та його пульсацій залежно від розмірів PM. Фактично, електромагнітний крутний момент збільшується лінійно з розміром PM, але це не відноситься до пульсацій крутного моменту.* Бібл. 22, табл. 2, рис. 16.

Ключові слова: **машина з нігтьовим полюсом, розмір постійного магніту, гібридні електромобілі, метод скінченних елементів, пульсація крутного моменту.**

Introduction. Claw pole machines (CPMs) are widely used in automotive applications; they are considered the energy of many electrical consumers of a vehicle. However, the mild hybrid vehicles technology allows energy transfer in both modes of operation. The system consists of recharging the battery and powering the electrical equipment in generator mode, and starting the vehicle in engine mode [1, 2]. In this case and unlike conventional vehicles, the diode bridge associated with the classic alternator is replaced by a voltage inverter transistor [1, 3].

A peculiarity of the CPMs is the structure of its rotor, the poles of which have the shape of a claw, hence its name. This particular structure makes claw alternators exceptionally competitive from an economic point of view, because they can be manufactured easily and quickly while having very good mechanical strength for operation at high rotational speed.

Traditionally, conventional CPMs use a single excitation winding which creates the rotor magnetic field. However, the high demand for electricity from automotive equipment such as security systems comfort and the use of starter-generator system leads to the consideration and introduction of permanent magnets (PMs).

Different rotor topologies containing PMs are used. The study presented in [4] concerning hybrid excitation CPMs for vehicles with 3D-FEM leads to increasing the air gap flux density. Thus, the electromagnetic torque of the CPM is increased and the torque ripples are reduced. In [5] the addition of PMs between the rotor claws allows a significant increase of more than 22 % in the output power of the CPM, but there is a non-linear relationship between the weight of the PMs and the torque when the PMs weight is considerable.

The equivalent magnetic circuit proposed and presented in [6] aims to visualize the influence of the type and volume of the PM (NdFeB) on the characteristics of a CPM, the proposed analytical method makes it possible to calculate the dimensions a PM which will create the desired electrical voltage. Therefore, in [7], a brushless PM claw pole motor with a soft magnetic composite is proposed. PMs are positioned on the claw pole surface and consequently, the optimal method applied gives an improvement of power density and torque density.

In order to eliminate the slip-ring and brush arrangement, a brushless electrically excited claw pole generator was proposed in [8, 9]; it had strong excitation magnetic performance, reduced excitation copper loss, and increased energy conversion efficiency. In [10], the ring PM structure is inserted in the stator yoke, and the stator and rotor are both claw-pole structures. Its power density has significantly increased. Another topology with skewed and non-skewed PMs in the claw-pole rotor fingers is presented in [10]. Results show that the CPM performances such as back-EMF value augments and the cogging torque vary when the skew angle increases.

Several techniques are used to introduce and place the PMs in the machine for hybrid excitation [11-15], however, the PMs placed between the claws destroy the excitation leakage flux in the rotor and, thus, improve the main flux for all speeds [1, 3, 4].

In this article, we examine how the PMs placed between the rotor claws affect the performance of the permanent magnet claw pole machine (PM-CPM) (Fig. 1) by taking into account the appropriate magnetization orientation and the PM's geometrical dimensions. An alternating arrangement of PMs between the claws of the rotor (Fig. 2) is required to have a possible sinusoidal waveform of the EMF. The magnetization of the PMs is chosen by carrying out a nonlinear 3D electromagnetic simulation of PM-CPM with consideration of the tangential and radial directions of magnetization.

Finally, in order to improve its power density, torque, and ripple torque, the impacts of PMs dimensions such as length and thickness on PM-CPM output torque are studied.

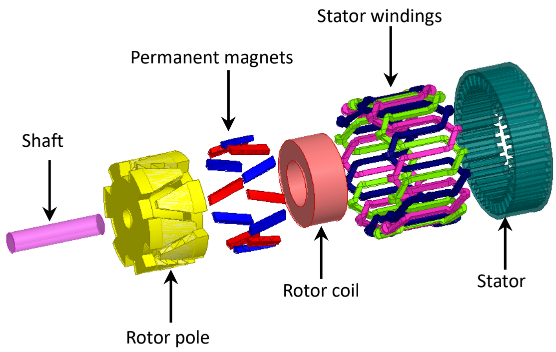

Fig. 1. Exploded view of the study machine

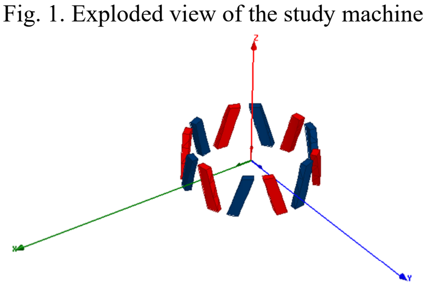

Fig. 2. PMs placement in the rotor and its arrangements

Electromagnetic model of PM-CPM. The claw pole rotor has an asymmetric structure relative to the length of the machine and produces 3D flux distributions. The model must take into account the components of the radial, tangential and axial field, the study therefore consists of a 3D model. PM-CPM analysis can take into account periodicity conditions to enable 3D simulation of a single pole pair. This pole pair structure is complex due to the shape of its two claws and its hybrid excitation. Thus, for electromagnetic design and analysis, a transient nonlinear 3D FEM model is used.

The mathematical model of the machine with hybrid excitation is described in reference d-q. The d-axis flux φ_d and the q-axis flux φ_q equations can be written as:

$$\varphi_d = L_d \cdot i_d + \varphi_r ; \quad (1)$$

$$\varphi_q = L_q \cdot i_q , \quad (2)$$

where i_d, i_q are the d-axis and q-axis stator current components; L_d, L_q are the d-axis and q-axis inductance respectively.

The rotor flux linkage φ_r is given as:

$$\varphi_r = L_{df} \cdot i_r + \varphi_{PM} , \quad (3)$$

where i_r is the rotor excitation coil current; φ_{PM} is the flux due to the PMs; L_{df} is the d-axis mutual inductance between the field winding and the armature winding.

The voltage equation of d-axis voltage component V_d and q-axis voltage component V_q are expressed as:

$$V_d = R_a \cdot i_d + \frac{\mathrm{d}\varphi_d}{\mathrm{d}t} - \omega \cdot \varphi_q ; \quad (4)$$

$$V_q = R_a \cdot i_q + \frac{\mathrm{d}\varphi_q}{\mathrm{d}t} - \omega \cdot \varphi_d , \quad (5)$$

where R_a is the stator winding phase resistance; ω is the angular velocity.

The torque T_e is given as:

$$T_e = \frac{3}{2} p \left(\varphi_d \cdot i_d + \varphi_q \cdot i_q \right), \quad (6)$$

where p is the number of pole pairs.

The above equation becomes:

$$T_e = \frac{3}{2} \cdot p \cdot \left[\left(L_d - L_q \right) \cdot i_d \cdot i_q + L_{df} \cdot i_r \cdot i_q + \varphi_{PM} \cdot i_q \right]. \quad (7)$$

Therefore, in the case for L_d close to L_q, the torque equation becomes:

$$T_e = \frac{3}{2} \cdot p \cdot i_q \cdot \varphi_r . \quad (8)$$

Equation (8) shows that the rotor flux is mainly responsible to create the electromagnetic torque. In this study, the parameters of the claw pole model used are shown in Table 1.

Table 1

The parameters of the machine

Rotor excitation current I_{ext}	4.5 A
Rotor coil number of conductor	400
Stator number conductor	12
Stator core length	32.5 mm
Stator number slots	36
External stator diameter	125.1 mm
Air gap length	0.8 mm
Rotor core diameter	93 mm
Number of poles	12
Rotor core length	52.4 mm

The PM's dimensions introduced between claws are shown in Table 2.

Table 2

PMs dimensions

Magnet length l	28.94 mm
Magnet width d	7.68 mm
Magnet thickness th	4.6 mm

Magnetization effect of PMs on PM-CPM. PMs magnetization orientation has an effect on PM-CPM performance at high or low speeds. However, different magnetization directions of PM and arrangements can generate different magnetic field distributions in the system as well as different motor performances [16]. These directly influence the quality of the air gap flux density distribution and affect the FEM induced, the producing torque, and the ripple torque [17, 18].

Furthermore, in electric motors with PMs, the waveform of the back EMF depends on the excitation and arrangement of the PMs and windings, the structure of the motor, and the pole/slot combinations. Thus, the designers want to get a purely sinusoidal or trapezoidal back-EMF waveform based on motor types and control [16]. The model proposed in this study can take into account two different directions of magnetization of the PMs [19], the application contents tangential magnetization and radial magnetization (Fig. 3).

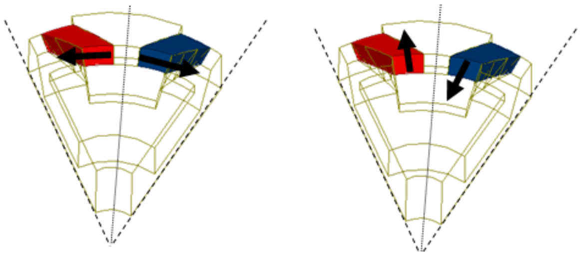

a *b*

Fig. 3. The orientation of PMs placed between the claws of a pole pair of the machine: *a* – tangential; *b* – radial

Electromagnetic field computation at 3000 rpm is carried out with the FEM. In order to analyze the effect of the magnetization orientation on the performance of the PM-CPM and to visualize only the impact of the excitation of the PMs, we consider the excitations of the rotor coils and those of the stator as zero. The PM-CPM magnets are oriented as shown in Fig. 3.

Figure 4 shows the magnetic flux distribution; we observe the difference repartitions of flux density between the tangential and radial magnetization. Furthermore, it can be seen that in the case of tangential magnetization the lines of flux pass directly into the adjacent claw and are channeled more into the magnetic circuit, which gives less leakage flux (Fig. 4,*a*). Whereas for the case of radial magnetization, the lines of flux pass in the vacuum existing between the claw and the rotor coil (Fig. 4,*b*), which does not help the principal flux and creates more leakage flux, and there will be a reduction in main flux, so the impact of radial magnetization is not significant.

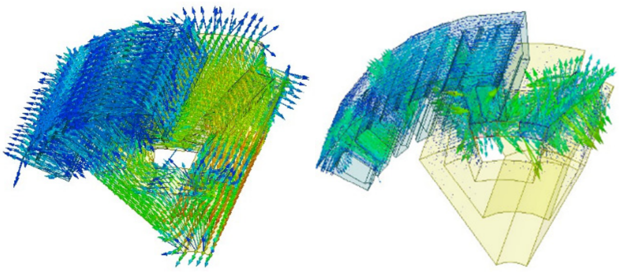

a *b*

Fig. 4. Magnetic field distribution:
a – tangential magnetization; *b* – radial magnetization

EMF considering only the magnetic excitation is shown in Fig. 5, the flux distributions in the tangential magnetization give induced three-phase voltage waveforms close to the sinusoid compared to that given by the radial magnetization.

One of the particular problems of electric machines with PMs is the shape of the cogging torque resulting from the interaction of the PMs and the teeth of the stator without even the stator winding being excited [20]. Also, a strong cogging torque can cause acoustic vibrations and noise.

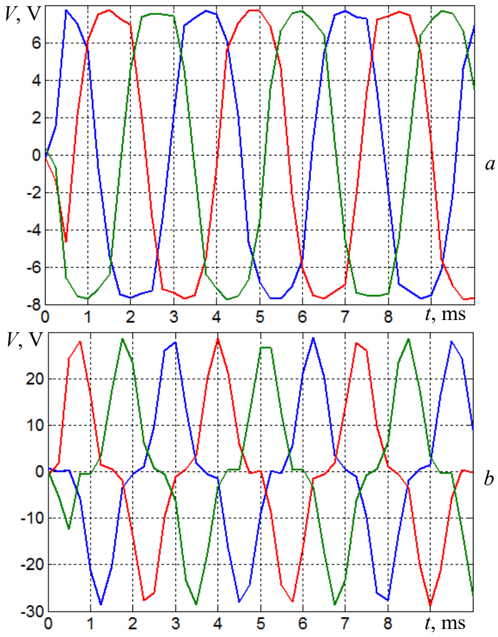

Fig. 5. Induced voltage for no-load and I_{ext} = 0:
a – tangential magnetization; *b* – radial magnetization

Figure 6 shows a comparison of the cogging torque between the two directions of magnetization in the case where the rotor excitation current is zero. We can see that the tangential magnetization gives a low cogging torque compared to that given by the radial magnetization. Then the tangential direction is strongly solicited.

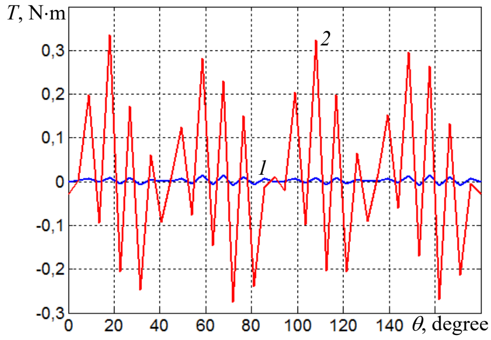

Fig. 6. Comparison cogging torque vs. rotational angle θ:
1 – tangential magnetization; *2* – radial magnetization

Hybrid excitation CPM performance. The rotor coil is preserved in case the regulator needs to change the battery voltage. For a hybrid excitation with a value I_{ext} = 4.5 A of the excitation rotor current and with PMs excitation, the calculation of the induced no-load voltage is illustrated in Fig. 7. The rates correspond to the 2 cases of magnetization tangential and radial magnetization. We can see that the RMS value of induced voltage in the case of tangential magnetization which is 32.3 V is greater than that in the case of radial magnetization which is 22.8 V. This comes down to the fact that in the case of the tangential direction the flux created by the PM is added to the flux created by the rotor coil and follows the same path. In addition, the use of inter-claw PMs with tangential magnetization makes it possible to reduce the leakage flux between claws.

Fig. 7. Induced voltage of one phase comparison for I_{ext} = 4.5 A:
1 – tangential magnetization; *2* – radial magnetization

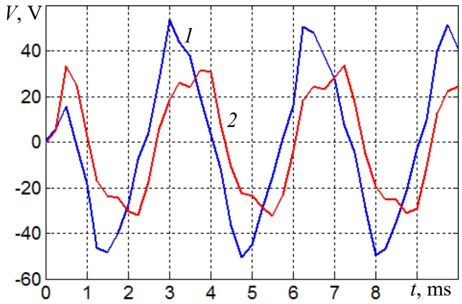

To better show the positive effect of tangential magnetization, Fig. 8 illustrates the induced voltage in the case of the presence of the PM with tangential orientation and in the case of the absence of the PM. We can see that the maximum value of the voltage increases almost twice.

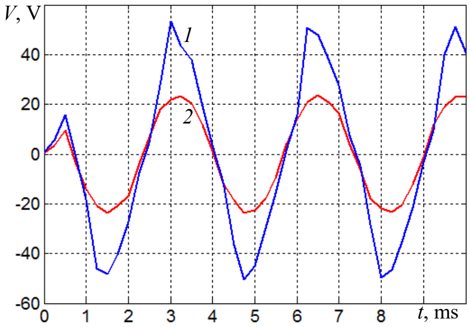

Fig. 8. Induced voltage comparison for I_{ext} = 4.5 A:
1 – with PMs tangential magnetization; *2* – without PMs

For load operation, the three-phase stator windings are fed by three-phase AC currents, the simulations with PM tangential magnetization and without PM of torque vs. rotor position at a nominal point such that stator current RMS value is 176.7 A and excitation current rotor is 4.5 A are given in Fig. 9. The structure without PMs gives an average torque of 21.2 N·m, after the introduction of PMs placed in inter-claws means that the torque increases because of the magnetic strength, and its average value is around 24.8 N·m. The result shows that the rotor design with PMs generates about 17 % more torque than the rotor design without PMs. We can see also that there are a lot of ripples, the ratio between the torque and its ripples is almost 16 % and 20 % for PMs rotor design and without PMs rotor design respectively.

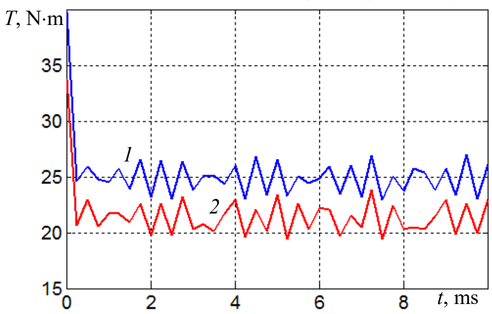

Fig. 9. Torque for I_{ext} = 4.5 A:
1 – with PM tangential magnetization; *2* – without PM

The torque as a function of the different values of the rotor current is presented in Fig. 10. We note the average torque value of 13.18 N·m at zero current excitation and we can be seen that the average torque increases linearly with the increase in excitation current due to the unsaturated claw rotor core. This variation becomes non-linear from 7 A of the excitation current due to rotor claws saturation. The electromagnetic torque depends mainly on the rotor flux, which verifies (8).

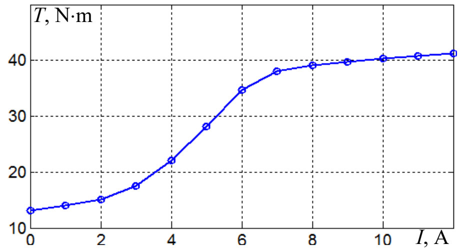

Fig. 10. Average torque vs. rotor current

To highlight the operation under load in steady state, the load angle is used as the parameter in this analysis of PM-CPM [21]. We assume that the instantaneous values of phase current and the load angle are known to investigate the electromagnetic torques.

The calculated values of the average torque with respect to load charge are shown in Fig. 11. In this case, we used a rotor excitation current I_{ext} = 7 A, in order to reach the magnetic saturation state of the machine. We can see the maximum value of 37.5 N·m of the electromagnetic torque corresponding to a load angle θ = 90°.

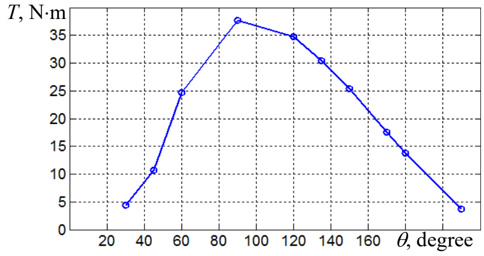

Fig. 11. Average torque vs load torque with for I_{ext} = 7 A

Parametric studies. In this study, the PMs placed between claws are applied with tangential magnetization to investigate the torque characteristics such as torque and ripple torque. The three-phase stator windings are fed by three-phase AC currents. As the PMs placed on the rotating part of the PM-CPM are responsible for the flux field, then a consideration of the dimensions of the PMs is taken into account. In particular, it takes into account the geometric length and the thickness of the PM (Fig. 12).

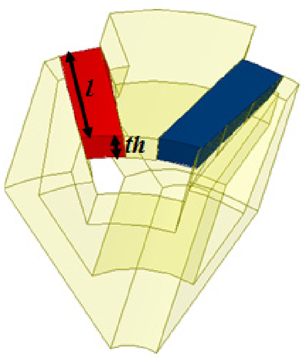

Fig. 12. PM dimensions variation

Varying magnet thickness. In this case, we vary the dimension of the magnet thickness *th* from 1.5 mm to 4.6 mm, when magnet length *l* keeps constant 30 mm.

Considering an optimal charging regime and for non-linear study state with rotor excitation current I_{ext} = 7 A, we notice that the torque increases with the increase of the PM thickness (Fig. 13).

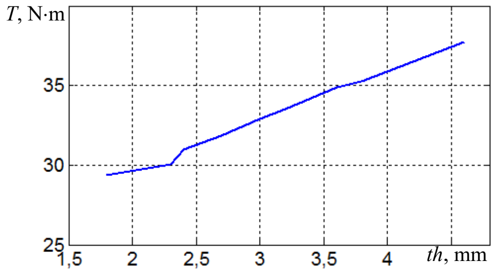

Fig. 13. Average torque vs. PM thickness with l = 30 mm

The ripple torque T_{ripp} can be defined as the rapport of the difference between the maximum torque and his minimum and the average value of torque [22], it is expressed as:

$$T_{ripp} = \frac{\max(T_e) - \min(T_e)}{\operatorname{avg}(T_e)} . \quad (9)$$

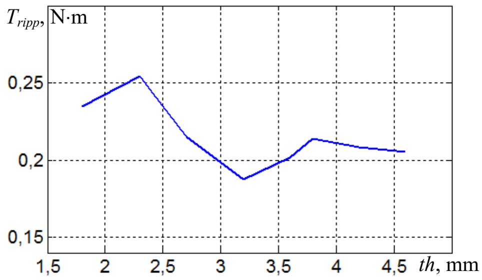

Fig. 14. Ripple torque vs. PM thickness

Varying magnet length *l*. For the same optimal conditions, we change l from 14 mm to 30 mm when the PM thickness th keeps constant 4.6 mm. We can see that when PM length increases the torque also increases (Fig. 15, 16).

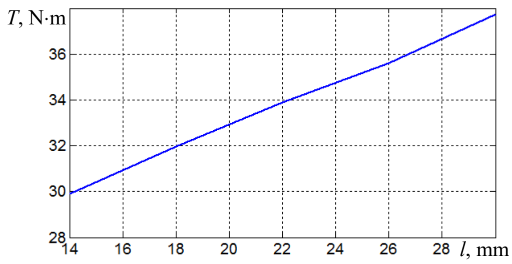

Fig. 15. Average torque vs. PM length with th = 4.6 mm

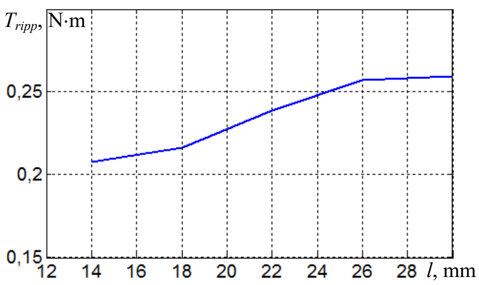

Fig. 16. Ripple torque vs. PM length

According to Fig. 13 – 16, we can see that the average torque increases with the increase in the size of the PMs. However, the impact on the torque ripples is not consistent; in fact, the torque ripples are minimal when the length of the PMs l is between 14 mm and 18 mm. Also, these ripples are minimal when the thickness th is between 2.9 mm and 3.6 mm. Then the torque ripples have a non-linear variation depending on the dimensions of the PMs.

Conclusions. In this paper, our first intention was to investigate the magnetization direction of PMs introduced between rotor claws. Two different PMs orientations were applied and presented different flux distributions, which in turn several motor performances.

As a result, the tangential magnetization direction shows the best performances of the permanent magnet claw pole machine (PM-CPM) such as a sinusoidal induced voltage and a best cogging torque. Furthermore, under optimal loading conditions, the CP-CPM with PMs tangential magnetization gives a higher average torque and a lower ripple torque compared to that given by the structure without magnets.

Finally, to know the impact of the size of the PMs of the CP-CPM on the torque characteristics, a parametric analysis of the variations in length and thickness of the PM showed evidence of an increase in magnetic force and torque. However, the torque ripples have a non-linear variation depending on the study parameters.

Conflict of interest. The authors declare that they have no conflicts of interest.

REFERENCES

1. Boldea I. Automotive Claw-Pole-Rotor Generator Systems. *Variable Speed Generators, Second Edition*, CRC Press, 2015, pp. 195-244 doi: https://doi.org/10.1201/b19293-7.

2. Ibrar A., Ahmad S., Safdar A., Haroon N. Efficiency enhancement strategy implementation in hybrid electric vehicles using sliding mode control. *Electrical Engineering & Electromechanics*, 2023, no. 1, pp. 10-19. doi: https://doi.org/10.20998/2074-272X.2023.1.02.

3. Bruyere A., Semail E., Bouscayrol A., Locment F., Dubus J.M., Mipo J.C. Modeling and control of a seven-phase claw-pole integrated starter alternator for micro-hybrid automotive applications. *2008 IEEE Vehicle Power and Propulsion Conference*, 2008, pp. 1-6. doi: https://doi.org/10.1109/VPPC.2008.4677668.

4. Li Y., Yu Z., Meng H., Wang J., Jing Y. Design and Optimization of Hybrid-Excited Claw-Pole Machine for Vehicle. *IEEE Transactions on Applied Superconductivity*, 2021, vol. 31, no. 8, pp. 1-4. doi: https://doi.org/10.1109/TASC.2021.3094433.

5. Upadhayay P., Kedous-Lebouc A., Garbuio L., Mipo J.-C., Dubus J.-M. Design & comparison of a conventional and permanent magnet based claw-pole machine for automotive application. *2017 15th International Conference on Electrical Machines, Drives and Power Systems (ELMA)*, 2017, pp. 1-5. doi: https://doi.org/10.1109/ELMA.2017.7955390.

6. Bachev I., Lazarov V., Zarkov Z. Analysis of the Influence of NdFeB Permanent Magnet's Type and Volume on the Characteristics of a PM Claw-pole Alternator. *2021 17th Conference on Electrical Machines, Drives and Power Systems (ELMA)*, 2021, pp. 1-6. doi: https://doi.org/10.1109/ELMA52514.2021.9502990.

7. Zhang Z., Liu H., Song T. Optimization Design and Performance Analysis of a PM Brushless Rotor Claw Pole Motor with FEM. *Machines*, 2016, vol. 4, no. 3, art. no. 15. doi: https://doi.org/10.3390/machines4030015.

8. Zhao X., Niu S., Ching T.W. Design and Analysis of a New Brushless Electrically Excited Claw-Pole Generator for Hybrid Electric Vehicle. *IEEE Transactions on Magnetics*, 2018, vol. 54, no. 11, pp. 1-5. doi: https://doi.org/10.1109/TMAG.2018.2823743.

9. Popa G.N., Maria Dinis C., Baciu I., Deaconu S.I. Automotive PM Surface Alternator, Analyse with Experiments. *2021 International Conference on Applied and Theoretical*

Electricity (ICATE), 2021, pp. 1-6. doi: https://doi.org/10.1109/ICATE49685.2021.9465009.
10. Zhao J., Hu C., Zhao Z., Tang M., Tang X. Suitable claw shape design for improving the magnetic properties of forged claw pole parts in generator. *IET Electric Power Applications*, 2021, vol. 15, no. 10, pp. 1331-1342. doi: https://doi.org/10.1049/elp2.12102.
11. Wardach M. Hybrid excited claw pole generator with skewed and non-skewed permanent magnets. *Open Physics*, 2017, vol. 15, no. 1, pp. 902-906. doi: https://doi.org/10.1515/phys-2017-0108.
12. Tong C., Zheng P., Wu Q., Bai J., Zhao Q. A Brushless Claw-Pole Double-Rotor Machine for Power-Split Hybrid Electric Vehicles. *IEEE Transactions on Industrial Electronics*, 2014, vol. 61, no. 8, pp. 4295-4305. doi: https://doi.org/10.1109/TIE.2013.2281169.
13. Geng H., Zhang X., Zhang Y., Hu W., Lei Y., Xu X., Wang A., Wang S., Shi L. Development of Brushless Claw Pole Electrical Excitation and Combined Permanent Magnet Hybrid Excitation Generator for Vehicles. *Energies*, 2020, vol. 13, no. 18, art. no. 4723. doi: https://doi.org/10.3390/en13184723.
14. Cao Y., Zhu S., Yu J., Liu C. Optimization Design and Performance Evaluation of a Hybrid Excitation Claw Pole Machine. *Processes*, 2022, vol. 10, no. 3, art. no. 541. doi: https://doi.org/10.3390/pr10030541.
15. Fujikura S., Hidaka Y. A Novel Rotor Structure of Claw-pole Motor Designed by Magnetomotive Force-based Simulation Method. *IEEJ Journal of Industry Applications*, 2020, vol. 9, no. 6, pp. 685-690. doi: https://doi.org/10.1541/ieejjia.20002397.
16. Bouakacha R., Ouili M., Allag H., Mehasni R., Chebout M., Bouchekara H.R.A. Measurement and three-dimensional calculation of induced electromotive force in permanent magnets heater cylinders. *Metrology and Measurement Systems*, 2022, vol. 29, no. 2, pp. 315-331. doi: https://doi.org/10.24425/mms.2022.140029.
17. Phyu H.N., Chao B. Effect of magnetization on high-speed permanent magnet synchronous motor design. *2012 15th International Conference on Electrical Machines and Systems (ICEMS)*, Sapporo, Japan, 2012, pp. 1-6.
18. Krishnan R. *Permanent Magnet Synchronous and Brushless DC Motor drives*. CRC Press, Taylor & Francis Group, 2017. 611 p. doi: https://doi.org/10.1201/9781420014235.
19. Boutora Y., Takorabet N., Ibtiouen R. Analytical model on real geometries of magnet bars of surface permanent magnet slotless machine. *Progress In Electromagnetics Research B*, 2016, vol. 66, pp. 31-47. doi: https://doi.org/10.2528/PIERB15121503.
20. Panchal T.H., Patel A.N., Patel R.M. Reduction of cogging torque of radial flux permanent magnet brushless DC motor by magnet shifting technique. *Electrical Engineering & Electromechanics*, 2022, no. 3, pp. 15-20. doi: https://doi.org/10.20998/2074-272X.2022.3.03.
21. Kurihara K., Wakui G., Kubota T. Steady-state performance analysis of permanent magnet synchronous motors including space harmonics. *IEEE Transactions on Magnetics*, 1994, vol. 30, no. 3, pp. 1306-1315. doi: https://doi.org/10.1109/20.297769.
22. Cao Y., Zhu S., Yu J., Liu C. Optimization Design and Performance Evaluation of a Hybrid Excitation Claw Pole Machine. *Processes*, 2022, vol. 10, no. 3, art. no. 541. doi: https://doi.org/10.3390/pr10030541.

Received 17.01.2024
Accepted 27.03.2024
Published 20.06.2024

A. Kimouche[1]*, Assistant Lecturer,*
M.R. Mekideche[1]*, Professor,*
M. Chebout[2]*, Associate Professor,*
H. Allag[1]*, Professor,*
[1] L2EI Laboratory, Department of Electrical Engineering,
Jijel University, Algeria,
e-mail: abdelghani.kimouche@univ-jijel.dz (Corresponding Author);
mohamed.mekideche@univ-jijel.dz; allag.hicham@univ-jijel.dz
[2] L2ADI Laboratory, Department of Electrical Engineering,
Djelfa University, Algeria,
e-mail: m.chebout@univ-djelfa.dz

How to cite this article:
Kimouche A., Mekideche M.R., Chebout M., Allag H. Influence of permanent magnet parameters on the performances of claw pole machines used in hybrid vehicles. *Electrical Engineering & Electromechanics*, 2024, no. 4, pp. 3-8. doi: https://doi.org/10.20998/2074-272X.2024.4.01